Yoon *et al. Egypt J Radiol Nucl Med (2023) 54:35*
https://doi.org/10.1186/s43055-023-00987-1

Egyptian Journal of Radiology and Nuclear Medicine

REVIEW

Open Access

Multidetector computed tomography evaluation of bladder lesions

Jin Woo Yoon, Sung Bin Park*, Eun Sun Lee and Hyun Jeong Park

Abstract

Background Urinary bladder tumors are the most common type of tumors detected in patients with gross hematuria. Multidetector computed tomography (MDCT) is an accurate method for detecting bladder lesions. This review aims to describe the features of MDCT and the possible values for distinguishing these lesions in the bladder.

Main body In this review, we discuss the role of MDCT in the evaluation of patients with bladder cancer and describe a broad spectrum of bladder lesions, including malignant bladder lesions beyond bladder cancer, benign bladder lesions, and diffuse bladder wall thickening.

Short conclusion Familiarity with the clinical presentations and imaging features of bladder lesions can lead to more accurate diagnosis and appropriate management.

Keywords Multidetector computed tomography, Urinary bladder neoplasms, Urinary bladder diseases, Early detection of cancer, Hematuria

Background

Urinary bladder lesions account for approximately 20% of all causes of hematuria and bladder tumors and are the most common types of tumors detected in patients with hematuria [1–3]. Multidetector computed tomography (MDCT) is an accurate examination for bladder lesion detection, with the sensitivity and positive predictive value of MDCT being 94% and 96%, respectively [1, 2]. The advantages of MDCT over conventional cystoscopy are patient tolerance and the ability to allow evaluation of the entire urinary tract and surrounding structures, as well as the bladder [1, 2]. MDCT can provide high accuracy and reliability comparable to conventional cystoscopy for bladder lesion detection and can be used as the primary diagnostic tool in patients with hematuria [1–4]. There is gap of knowledge in literature and limitations of MDCT in evaluation of bladder lesions.

In this review, we discuss the role of MDCT in the evaluation of bladder lesions and discuss broad spectrum bladder lesions ranging from benign to malignant.

Main text

MDCT for the detection of bladder lesions

Bladder CT scans were classified as conventional CT, CT cystography, and virtual cystoscopy [1].

On conventional CT, urothelial-phased scan (arterial or early portal phase) or delayed excretory-phased scans were used. Currently, both urothelial (portal) and excretory (delayed) phase CT scans are used to evaluate bladder lesions to improve sensitivity [1, 2]. Because most bladder cancers show early enhancement (with maximal enhancement at 60–80 s after contrast administration), a 70-s delayed urothelial phase has been found to show satisfactory contrast between a bladder tumor and the rest of the bladder wall and the highest diagnostic accuracy. Bladder lesions are usually revealed as intraluminal hyper-enhanced lesions or hyper-enhanced wall thickening compared with the normal bladder wall on urothelial

*Correspondence:
Sung Bin Park
pksungbin@paran.com
Department of Radiology, Chung-Ang University Hospital, Chung-Ang University College of Medicine, 102, Heukseok-Ro, Dongjak-Gu, Seoul 06973, Republic of Korea

phase images or filling defects on excretory phase images (Figs. 1, 2) [1, 2]. CT can also be useful for monitoring in patients who have been previously treated for bladder cancers (Fig. 2). Furthermore, MDCT enables high-quality multiplanar reformation (MPR) owing to thinner collimation and faster scanning, thereby greatly improving scan resolution, and allowing reconstruction in any desired plane, leading to better sensitivity for the detection of small bladder lesions (Fig. 3) [1].

However, a false-negative diagnosis of bladder cancer can be made using MDCT. Small and flat lesions, such as carcinoma in situ, may not present as filling defects and show only a little or no focal bladder wall thickening or abnormal enhancement (Fig. 3). Furthermore, bladder lesions located near the bladder base may be difficult or impossible to differentiate from an enlarged prostate or periurethral tissue. Causes of false-positive results include prostate enlargement, post-treatment, or inflammatory changes, trabeculated bladder, and blood clots [5, 6].

The MDCT protocol at our institution for evaluating patients with suspected bladder lesion includes an unenhanced scan, urothelial-phase scan, delayed excretory-phase scan and coronal maximal intensity projection view during the excretory-phase. A 64-slice CT scanner (including Brilliance 64; Philips Health Systems, Cleveland, OH, USA) was used. Patients were instructed not to void for at least one hour before the examination to obtain adequate bladder distension. During unenhanced scanning, adequate bladder distension was assessed. After unenhanced CT images were obtained, intravenous contrast agent (Iobrix® 300, Iohexol; Taejoon Pharm, Seoul, Korea) was administered by a power injector at 2 mL/kg of body weight and 3 mL/s. The urothelial-phase scan covered the entire bladder at the 70-s scanning delay. The parameters for the urothelial-phase scan were as follows: X-ray tube voltage: 100–120 kV; tube current: 130–250 mAs; beam collimation: 64 × 1.25 mm; gantry rotation time:0.33 s; matrix: 512 × 512; field of view: 320–400 mm; effective section thickness: 2–3 mm; reconstruction interval: 2 mm. The data were automatically reconstructed with iDose reconstruction technique, level 5 (Philips Healthcare).

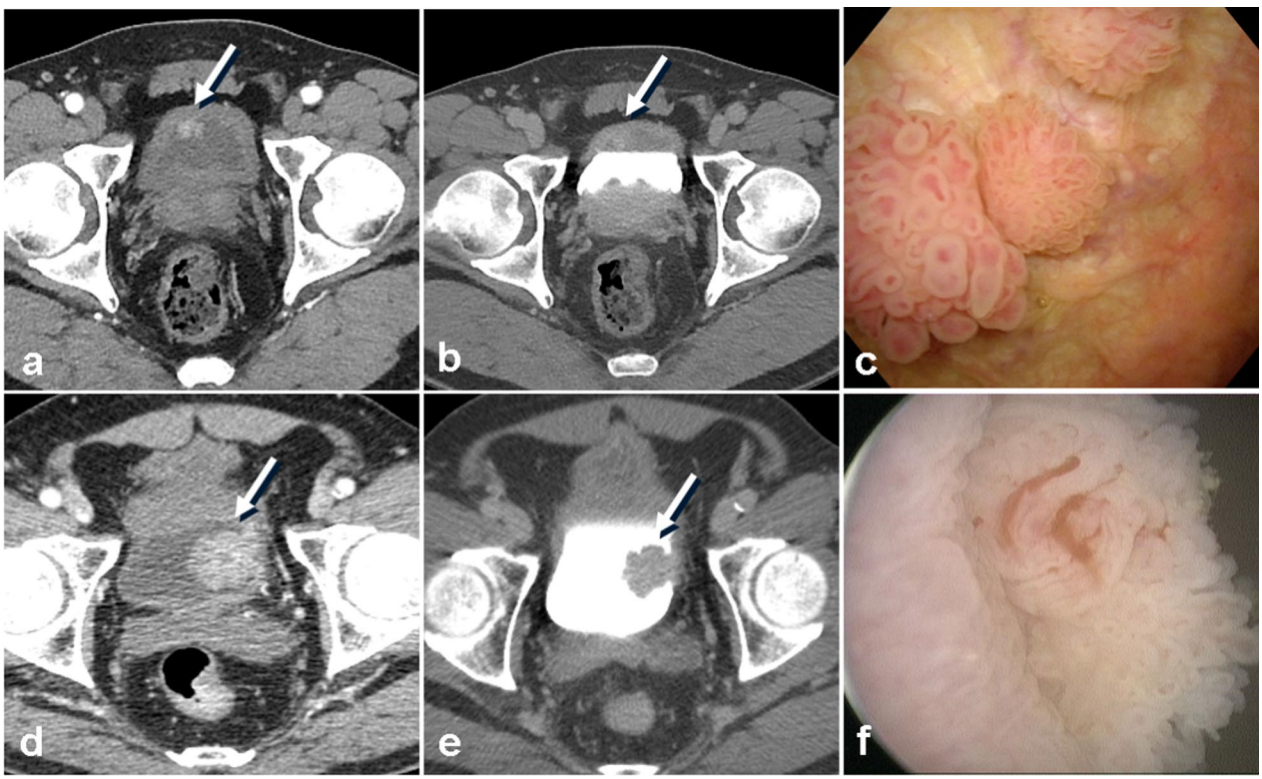

Fig. 1 Urothelial (portal) and excretory (delayed) phase scans of CT urography in two patients of urothelial carcinoma. **a** Axial urothelial phase CT image of a 63-year-old man obtained at 70 s after bolus intravenous contrast material injection shows a small hyper-enhancing polypoid mass (arrow) that enhances more than normal bladder mucosa. **b** Axial excretory phase CT image shows the enhancing bladder lesion (arrow) but is less pronounced compared to the urothelial phase. **c** The nodule was also identified using conventional cystoscopy. **d** Axial urothelial phase CT image of a 74-year-old man shows an intraluminal hyper-enhancing mass (arrow) on the left wall of the bladder. **e** Axial excretory phase CT reveals the mass as a filling defect (arrow) within the bladder lumen. **f** The nodule was also detected using conventional cystoscopy

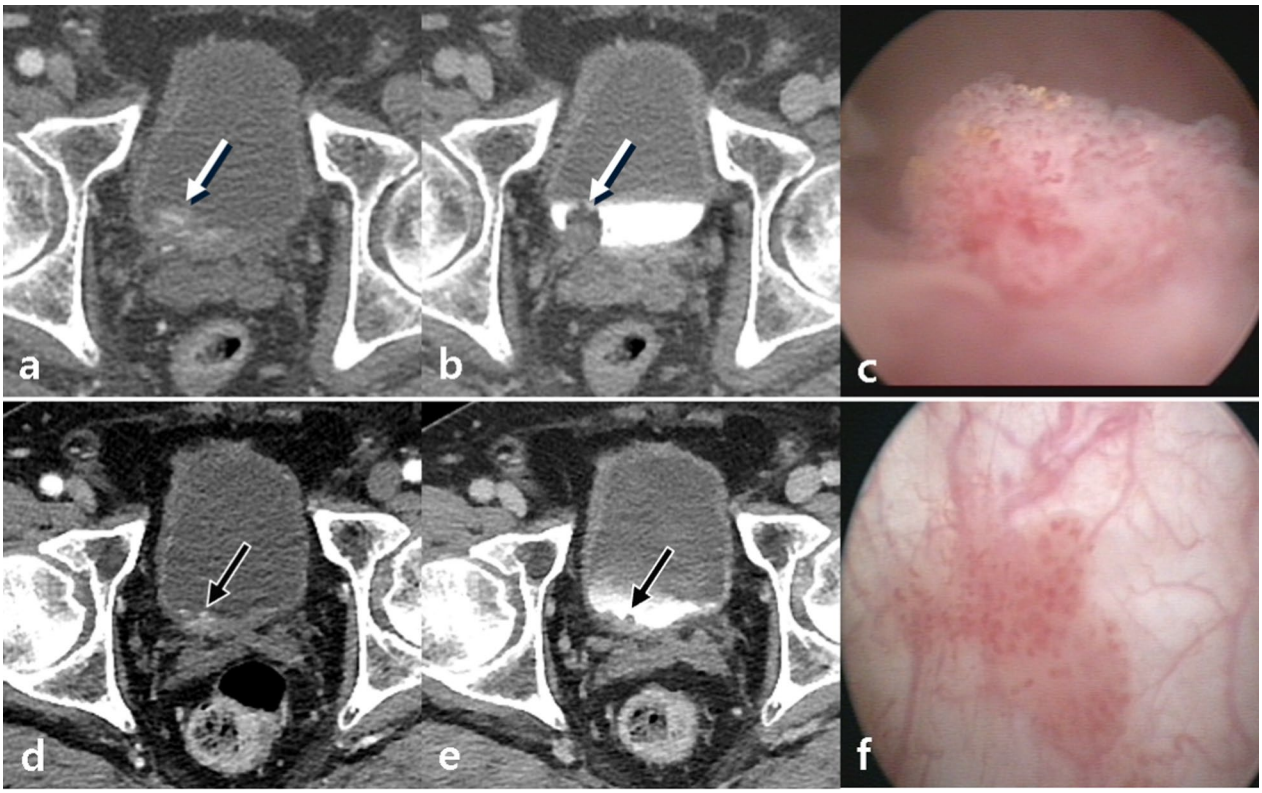

Fig. 2 Urothelial and excretory phase scans of CT urography in initial and recurred urothelial carcinomas. **a** Axial urothelial phase CT image of a 70-year-old man shows a small hyper-enhancing polypoid mass (arrow) that enhances more than normal bladder mucosa. **b** Axial excretory phase CT image shows the enhancing bladder lesion (arrow) but is less pronounced compared to the urothelial phase. **c** The nodule was also identified using conventional cystoscopy. Taken at the 6-month follow-up after transurethral resection of the bladder tumor, this axial urothelial phase CT image **d** shows an intraluminal hyper-enhancing mass (arrow) on the posterior wall of the bladder, the same as the initial tumor site. **e** Axial excretory phase CT of the patient shows that the mass is a filling defect (arrow) within the bladder lumen. **f** The nodule was detected using conventional cystoscopy

CT cystography and virtual cystoscopy

CT cystography and virtual CT cystoscopy are invasive procedures that require the Foley catheterization and active bladder distension [1, 2]. Moreover, it offers little advantage over performing flexible cystoscopy. Nevertheless, the sensitivities are not impressively better than those obtained in evaluating bladder CT [1].

CT cystography should be considered in patients with suspected bladder injury after initial CT scan of the abdomen and pelvis [7]. To obtain an optimal CT cystography scan, drain urine via catheter to remove unopacified urine from the bladder prior to instilling contrast material. Typically, commercially available prediluted contrast or admixed ionic/nonionic intravenous contrast diluted at a 1:10 ratio with normal saline (approximately 3–5% iodinated solution) is instilled via gravity-drip infusion. A container of contrast is hanged 40 cm above bladder to generate adequate pressure and connected to the catheter. The bladder is filled with contrast until flow of contrast stops, bladder distension is uncomfortable to patient, or 350 mL of contrast has been instilled. Image acquisition with thin section imaging allows for isotropic voxel acquisition and optimal multiplanar reformats. Added coronal and sagittal reconstructions have shown improved detection of bladder injuries, that could potentially be missed on axial images [7]. Delayed post drainage reimaging is generally not performed.

CT virtual cystoscopy can be of great value as a complementary tool when conventional cystoscopy is not feasible. The creation of virtual cystoscopy can be obtained via 3D volume rendering technique. The procedure involves bladder distension, usually using air insufflation technique prior to CT scan. A three-way Foley catheter is inserted into the bladder to achieve complete voiding. The bladder is then distended by insufflating 350–500 cc of room air with syringes, according to the patient's tolerance. Helical CT scans are obtained with patients in both the supine and prone position to prevent possible residual fluid obscuring small mural lesions. Post-processing CT data obtained are transferred to a workstation

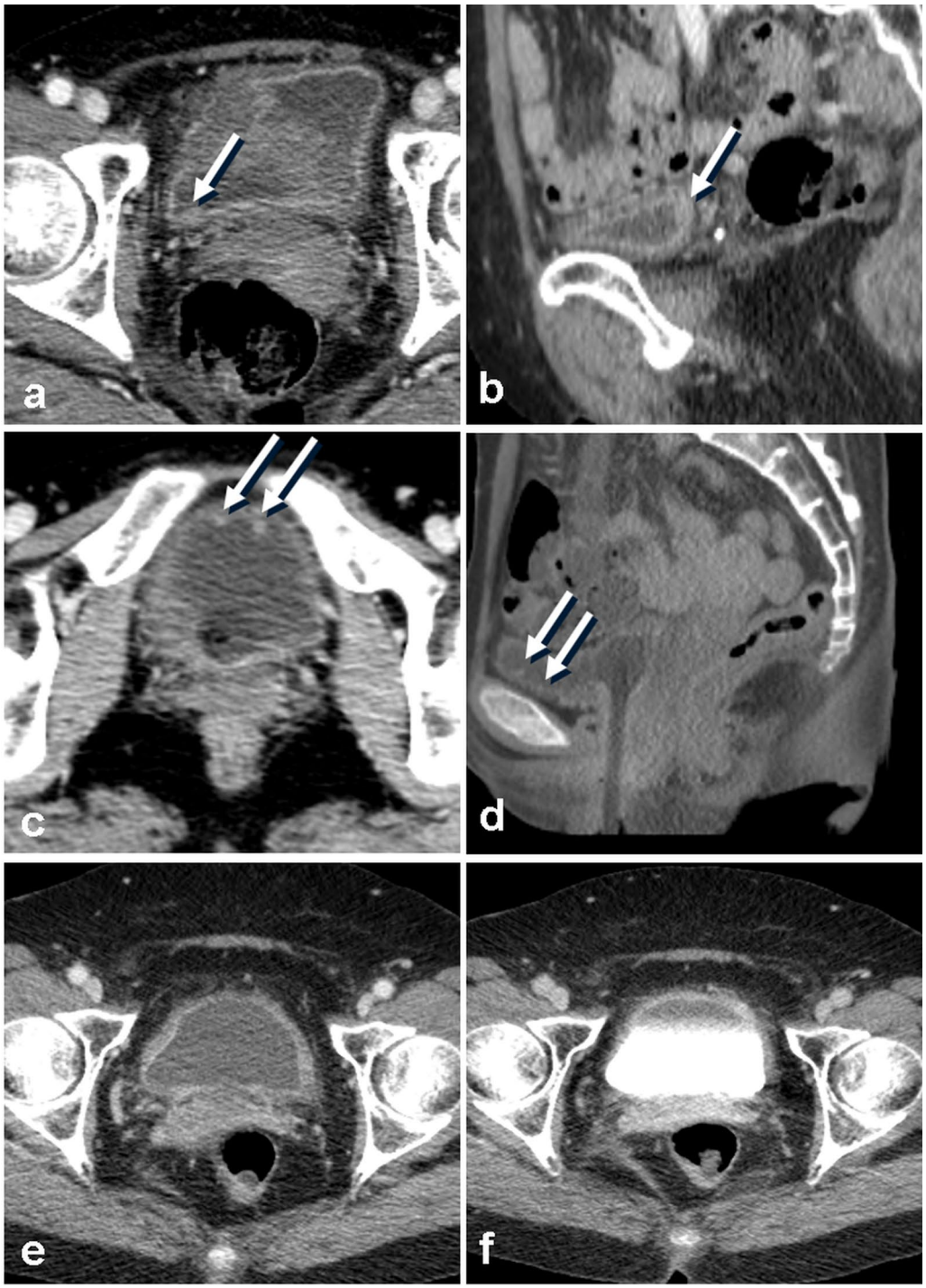

Fig. 3 CT detection of small and flat bladder lesions multiplanar reformation (MPR) in three patients of urothelial carcinoma. Axial (**a**) and sagittal (**b**) urothelial phase CT images of a 73-year-old woman showing an enhanced area of focal wall bladder thickening (arrows). Axial (**c**) and sagittal (**d**) urothelial phase CT images of a 58-year-old woman showing two tiny enhancing lesions (arrows) on the anterior wall of the bladder. Axial urothelial (**e**) and excretory (**f**) phase CT images of a 71-year-old woman showing subtle diffuse or segmental mucosal enhancement of the bladder without filling defects. The patient was diagnosed with urothelial carcinoma in situ on histopathological examination. Small or flat lesions are more difficult to detect with CT

equipped with software for interactive intraluminal navigation with a surface-rendering algorithm. Navigation inside the bladder can be performed at 360 degrees from different directions to assess the bladder wall and lumen. If any abnormal lesion is detected, it should be fully evaluated in all projections. Virtual cystoscopy is a minimally invasive technique that allows visualization of the entire bladder within the lumen, even in areas inaccessible with conventional cystoscopy. Limitations of virtual cystoscopy include its inability to detect color changes of the mucosa and obtain tissue biopsy [2, 4].

Malignant bladder lesions

Bladder cancer

According to the 2022 World Health Organization (WHO) classification of the urinary and male genital tumors [8], bladder cancers are mainly classified as invasive urothelial carcinoma, squamous cell carcinoma, adenocarcinoma and urachal carcinoma (Table 1). Mesenchymal, hematolymphoid, neuroendocrine, metastatic and genetic syndrome–related tumors are splitted by tumor lineages of differentiation that may occur in different urinary tract locations. Invasive urothelial carcinoma, also known as transitional cell carcinoma, is the most common urinary tract cancer, accounting for 95% of bladder cancer cases, and has a propensity to be multicentric (up to 40% of cases). Bladder cancers have a variety of different CT appearances, such as intraluminal papillary or nodular mass, asymmetric or focal wall thickening, small filling defects (Figs. 1, 2), and less frequently diffuse wall thickening (Fig. 3) [5]. Diffuse bladder wall thickening is usually caused by benign abnormalities, including cystitis, bladder outlet obstruction, overactive bladder, and neurogenic bladder [5, 9]. Incidentally detected bladder wall thickening on CT can be suggestive of bladder malignancy (Fig. 3), particularly focal bladder wall thickening rather than diffuse. Therefore, further workup, including cystoscopy and urine cytology, should be performed to assess bladder malignancy [9].

Nonetheless, squamous cell carcinoma tends to be sessile rather than papillary, compared with urothelial carcinoma (Fig. 4). Furthermore, nonurachal adenocarcinoma

Table 1 The 2022 WHO classification of urinary tract tumors

Urothelial tumors	
Noninvasive urothelial neoplasms	Urothelial papilloma Urothelial papilloma, inverted Papillary urothelial neoplasm of low malignant potential Noninvasive papillary urothelial carcinoma, low grade Noninvasive papillary urothelial carcinoma, high grade Urothelial carcinoma in situ
Invasive urothelial neoplasms	Invasive urothelial carcinoma
Squamous cell neoplasms of the urinary tract	
	Squamous papilloma
Squamous cell carcinomas of the urinary tract	Verrucous carcinoma Pure squamous carcinoma of the urothelial tract
Glandular neoplasms	
Adenomas	Villous adenoma Tubular adenoma Tubulovillous adenoma
Adenocarcinomas	Adenocarcinoma, NOS Enteric adenocarcinoma Mucinous adenocarcinoma Mixed adenocarcinoma Signet ring cell adenocarcinoma Adenocarcinoma in situ
Urachal and diverticular neoplasms	
	Urachal carcinoma Invasive urothelial carcinoma
Urethral neoplasms	
Urethral accessory gland carcinomas	Carcinoma of Littré glands Carcinoma of Skene glands Carcinoma of Cowper glands
Tumors of Mullerian type	
	Clear cell carcinoma Endometrioid carcinoma

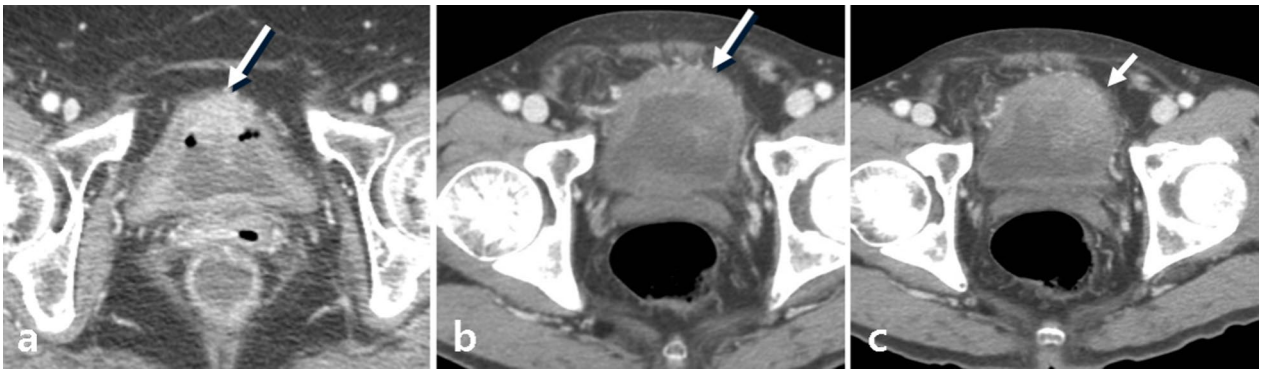

Fig. 4 Two cases of bladder cancer. **a** Axial urothelial phase CT image of a 67-year-old female patient with bladder squamous cell carcinoma shows an enhancing sessile or nodular mass (arrow) in the anterior wall of the bladder. **b**, **c** Axial contrast-enhanced CT images of a 68-year-old male patient with bladder adenocarcinoma show diffuse bladder wall thickening (arrow) along the anterior wall of the bladder and a large irregular enhancing intramural mass within the bladder. There is irregular soft tissue stranding (small arrow) from tumor invasion into the perivesical fat

tends to show diffuse bladder wall thickening, perivesical fat stranding (Fig. 4), lymphadenopathy, and invasion of adjacent organs. Urachal adenocarcinoma is characteristically located at the midline of the bladder dome, and an infraumbilical soft tissue mass with calcification strongly suggests urachal adenocarcinoma [10].

It is difficult to distinguish superficial bladder cancer (T1) from muscle-invasive bladder cancer (T2) using MDCT. Magnetic resonance imaging (MRI) can distinguish muscle-invasive from non-muscle-invasive tumors with accurate local staging. Vesical Imaging-Reporting and Data System (VI-RADS) score is a new diagnostic modality used for the prediction of tumor aggressiveness and therapeutic response [2]. Furthermore, the detection of microscopic perivesical tumor invasion (stage T3a disease) using MDCT can be challenging. The diagnosis of stage T3b disease (macroscopic perivesical tissue invasion) can also be challenging because perivesical soft tissue stranding is a nonspecific finding and can be due to tumor extension or merely reactive change or edema [5].

Leiomyosarcoma

Leiomyosarcoma is the most common malignant mesenchymal tumor originating in the bladder in adults. It accounts for less than 1% of all bladder malignancies, and its risk factors include systemic chemotherapy with cyclophosphamide and radiation therapy [10].

Imaging findings of leiomyosarcoma can mimic those of benign leiomyoma, and it can be difficult to distinguish leiomyoma from leiomyosarcoma even with MRI [10]. However, if the mass is large, heterogeneous signal intensity on T2-weighted images is seen in leiomyosarcoma due to necrosis. Furthermore, poorly circumscribed margins and invasion of adjacent structures can also be observed (Fig. 5) [10].

Rhabdomyosarcoma

Rhabdomyosarcoma is the most common bladder tumor in children and generally occurs before the age of 10 years. It affects boys more than girls in a 3:1 ratio [10].

Rhabdomyosarcoma typically shows large, nodular filling defects or masses in polypoid or grape-like shapes, often referred to as 'sarcoma botryoides.' These tumors often involve the bladder base, are associated with urinary tract obstruction, and may become difficult to distinguish from a prostate tumor. Grape-like intraluminal masses of the bladder on imaging in pediatric patients strongly suggest rhabdomyosarcoma [10].

Lymphoma

As no lymphoid tissue is normally found in the bladder, primary bladder lymphoma is extremely rare, but secondary involvement of the bladder can occur in 10–25% of patients with systemic lymphoma and leukemia [10, 11]. Primary lymphoma of the bladder is either the low-grade B-cell lymphoma of mucosa-associated lymphoid tissue (MALT) or diffuse large B-cell lymphoma (DLBCL) [10, 11]. Typically affecting adults aged > 60 years, 75% are females with associated chronic cystitis, and the initial symptoms include hematuria, dysuria, and abdominal or back pain [11].

The imaging features are nonspecific and include solitary bladder masses (70%), multiple masses (20%), and diffuse bladder wall thickening (10%) (Fig. 6) [2, 10, 11].

Benign bladder lesions

Benign bladder lesions can be classified as epithelial tumors, mesenchymal tumors, and non-tumorous bladder lesions. Benign bladder neoplasms represent less than

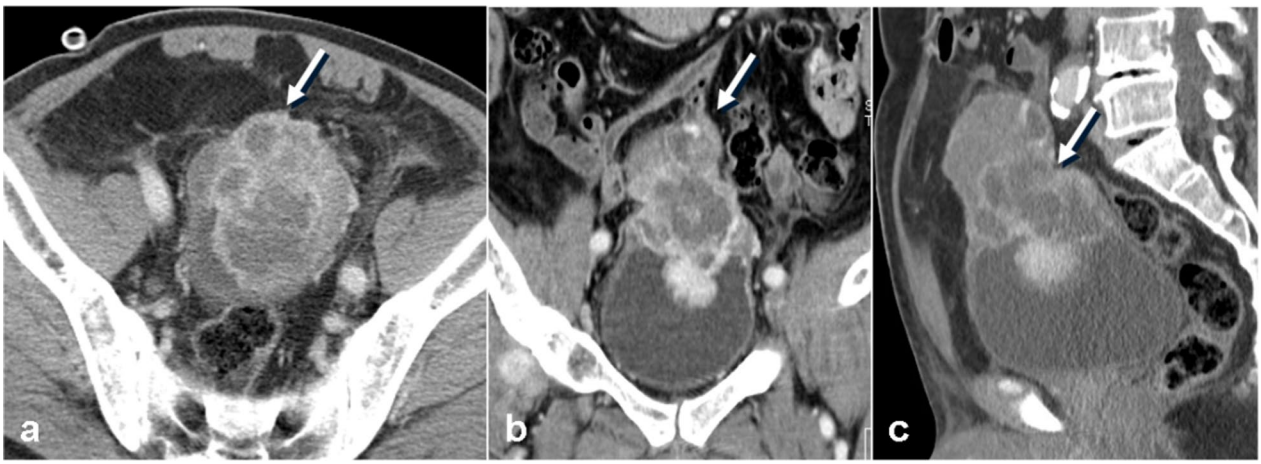

Fig. 5 A 67-year-old male patient with bladder leiomyosarcoma. Axial (**a**), coronal (**b**), and sagittal (**c**) contrast-enhanced CT images showing a large, poorly circumscribed, heterogeneously enhancing mass (arrows) on the dome of the bladder wall

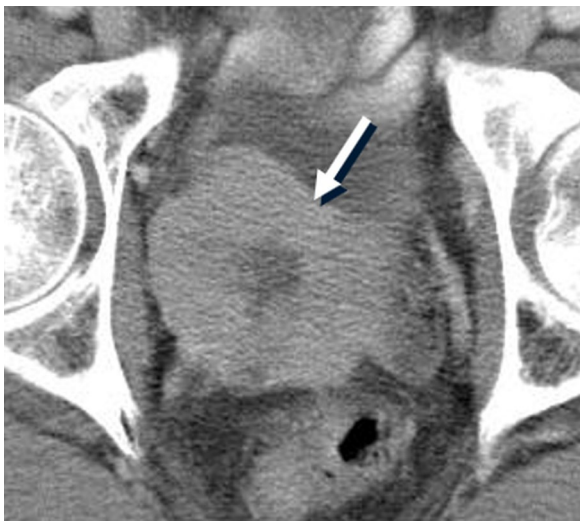

Fig. 6 A 60-year-old male patient with bladder lymphoma. Axial contrast-enhanced CT image showing marked circumferential wall thickening of the bladder (arrow)

1% of bladder tumors. There is a significant overlap in the clinical features and radiologic findings of benign bladder neoplasms, which often require a biopsy for diagnosis.

Leiomyoma

Leiomyoma is the most common mesenchymal tumor of the bladder and is mainly found in the trigone of the bladder. Nevertheless, bladder leiomyoma is a rare, benign tumor with an incidence rate lower than 0.5% among all types of bladder tumors [10, 12]. The incidence of bladder leiomyoma in females is twice that in males. Furthermore, patients aged approximately 50 years have the highest risk [12]. Bladder leiomyomas can be intravesical (60%), intramural (10%), or extravesical (30%) [10]. Among these three types of bladder leiomyomas, the intravesical forms are most likely to cause irritation, obstruction, or bleeding symptoms because they protrude into the lumen of the bladder.

Imaging findings include well-delineated, smooth, and uniform solid masses of the bladder wall, similar to those of the uterine counterpart (Fig. 7) [10]. Bladder leiomyoma can also manifest as a cystic component, indicating degeneration.

Papilloma and papillary urothelial neoplasms of low malignant potential (PUNLMP)

Papillary lesions of the bladder urothelium include papilloma, inverted papilloma, PUNLMP, and papillary urothelial carcinoma [10].

PUNLMP is a low-grade, small, solitary neoplasm with no invasion or metastasis, and it can be difficult and subjective to distinguish it from low-grade carcinoma (Fig. 8) [10]. Surveillance is required because the recurrence rate of PUNLMP is approximately 35% and progresses at approximately 10% [13].

Cystitis cystica and cystitis glandularis

Cystitis cystica and cystitis glandularis are chronic inflammatory disorders associated with metaplasia caused by chronic irritation or infection. The urothelium proliferates into the lamina propria, forms a solid nest called Brunn's nest, and then degenerates into cystic deposits, resulting in cystitis cystica or differentiation into the mucin-secreting glandular structure of cystitis glandularis [14]. They predominantly occur in the bladder neck, and trigone region of the bladder [15]. They may occur at any age, and there is a slight male predominance

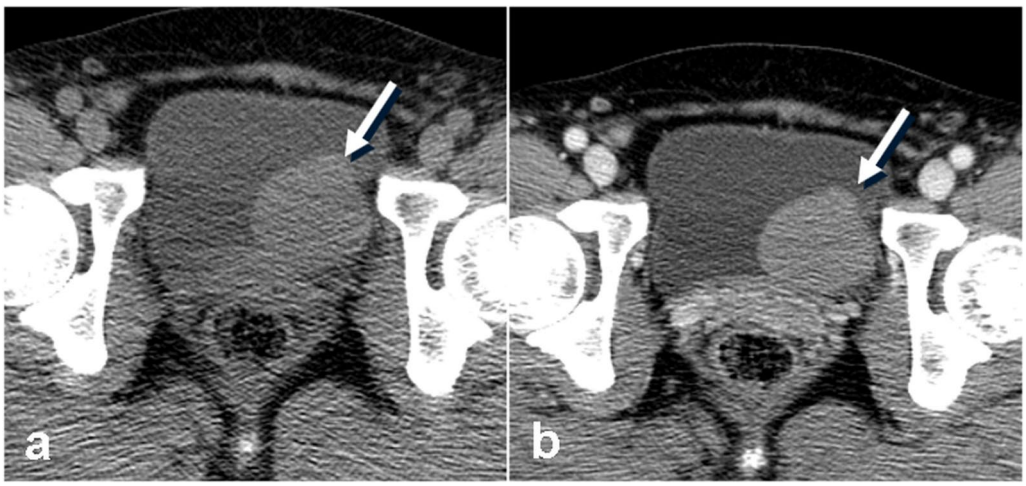

Fig. 7 A 57-year-old female patient with bladder leiomyoma. Axial non-contrast **a** and contrast-enhanced **b** CT images showing a smooth homogenous enhancing solid mural mass of the bladder (arrow), similar in appearance to uterine leiomyoma

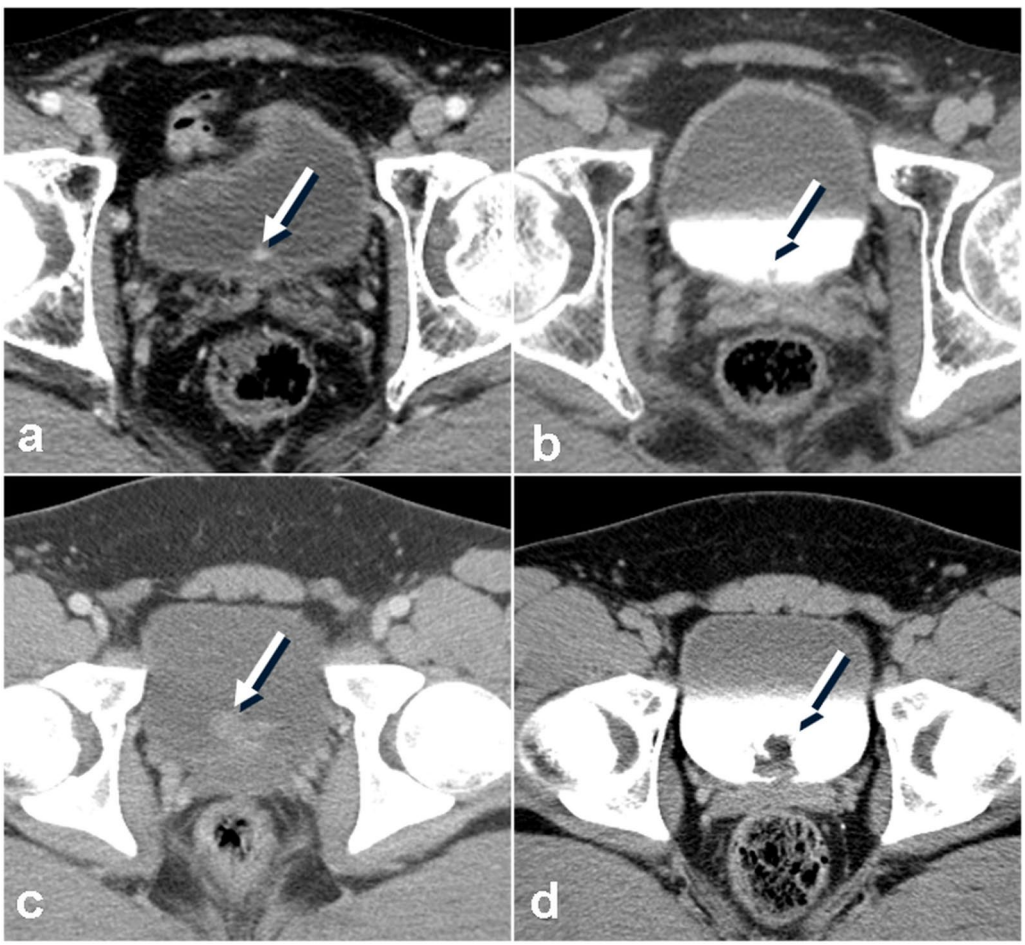

Fig. 8 Two cases of bladder papilloma and papillary urothelial neoplasm of low malignant potential (PUNLMP). Axial urothelial phase **a** CT image of a 60-year-old male patient with bladder papilloma showing a tiny enhancing lesion (arrow) on the trigone of the bladder and also demonstrating a filling defect (arrow) on the excretory phase (**b**) CT image. Axial urothelial phase **c** of a 19-year-old male patient with PUNLMP and excretory phase (**d**) CT images showing an irregular polypoid enhancing lesion and filling defect (arrows) in the bladder mimicking bladder cancer

[15]. Some authors have reported that these masses can progress to adenocarcinoma of the bladder; however, this remains contentious [15].

Cystitis cystica and cystitis glandularis manifest as single or multiple masses that vary in number and size, which may result in a cobblestone pattern, mimicking bladder cancer on imaging (Fig. 9) [14].

Endometriosis

Bladder endometriosis is uncommon. However, the bladder is the most common site for endometriosis within the urinary tract. Bladder endometriosis has only been reported in premenopausal women [14]. Bladder implants typically occur in the posterior wall of the bladder, including the dome, trigone, or vesicouterine pouch.

Imaging findings typically show a submucosal mass located posteriorly in the bladder, with variable protrusion into the bladder lumen, producing an obtuse bulge (Fig. 10). They are rarely isolated, and other endometriosis foci in the pelvis help to correct the diagnosis [14].

Paraganglioma

Paraganglioma of the bladder is an exceedingly rare pheochromocytoma arising outside the adrenal gland, which rarely develops in the bladder [10]. It constitutes less than 6% of all paragangliomas and 0.06% of all primary bladder tumors [16, 17]. It has a predilection age of 30–50 years, with no sex differences [17]. A characteristic 'micturition attack,' such as elevated blood pressure, headache, or syncope during micturition, occurs in 50% of patients due to

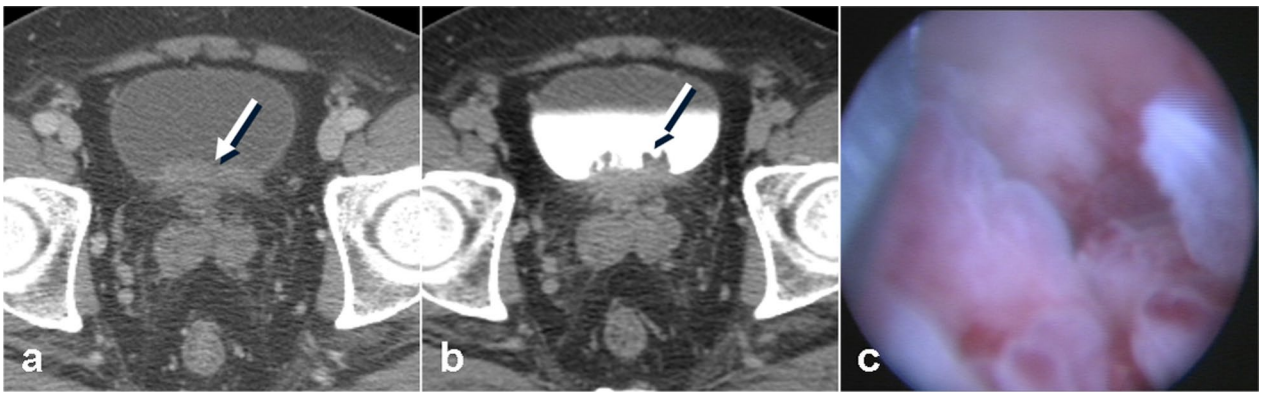

Fig. 9 A 49-year-old male patient with cystitis glandularis. Axial urothelial (**a**) and excretory (**b**) phase CT images showing multiple polypoid intramural enhancing and filling defect lesions (arrows) in the bladder. **c** Cystoscopy showing a cobblestone appearance of the mucosa with polypoid masses

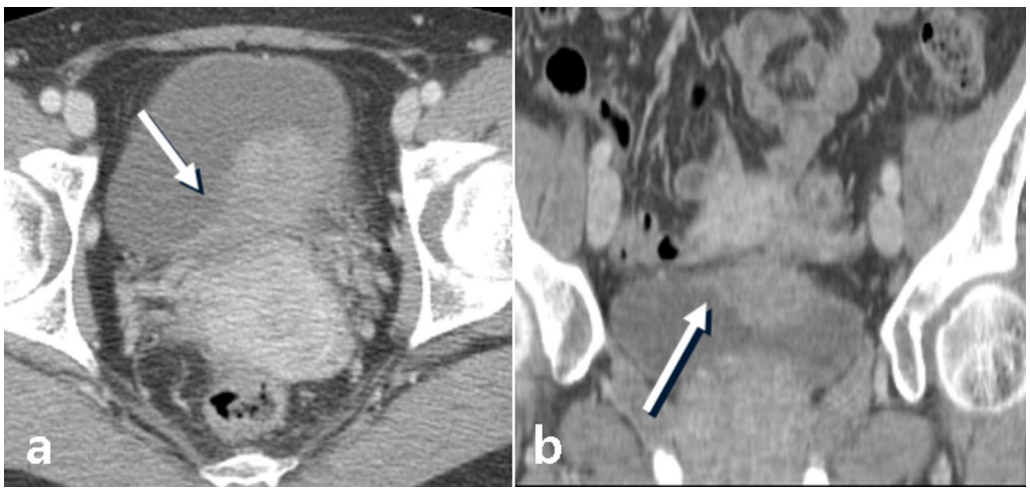

Fig. 10 A 37-year-old female patient with bladder endometriosis. Axial (**a**) and coronal (**b**) urothelial phase CT images showing a solid, well-marginated enhancing mass at the dome of the bladder. Note the obtuse angle of the mass from the bladder wall (arrow)

catecholamine release. Functional paraganglioma should be considered when the tumor is > 3 cm [16]. Most are sporadic but can also occur due to hereditary syndromes such as neurofibromatosis, von Hippel–Lindau syndrome, and Sturge–Weber syndrome [10].

A bladder paraganglioma is usually a well-marginated, submucosal, solid solitary mass (Fig. 11) and can occur anywhere in the bladder, but most commonly in the dome or trigone [16]. It often attaches to the bladder wall with a broad base. It may be pathologically based on its tendency to infiltrate and grow along the muscularis [17]. Marked enhancement, peripheral ring calcification, and high signal intensity on T2-weighted images are key imaging features of bladder paragangliomas (Fig. 11) [10].

Inflammatory myoblastic tumor

An inflammatory myoblastic tumor (IMT) is a spectrum of nonneoplastic myofibroblastic proliferation with inflammatory infiltrates and myxoid components [14, 18]. IMTs of the urinary system are relatively rare, and the bladder and prostate are the most common sites of their occurrence [18]. Bladder IMTs typically occur in younger individuals, particularly females, but rarely in children [19]. The clinical symptoms of bladder IMT include hematuria, frequent micturition, and painful urination [18]. Moreover, in some studies, urinary system IMTs were associated with a history of pelvic surgery [19].

On imaging evaluation, IMT usually appears as a single intraluminal or exophytic bladder mass, which may be ulcerated or show ring enhancement (Fig. 12). IMTs mainly occur in the superior or front wall of the bladder [19]. The pathognomonic feature of ring-like enhancement is produced by necrosis in the central region and spindle cells, myxoid components, vessels, and inflammatory cells in the periphery. The observation that polypoid nodules on the bladder walls show

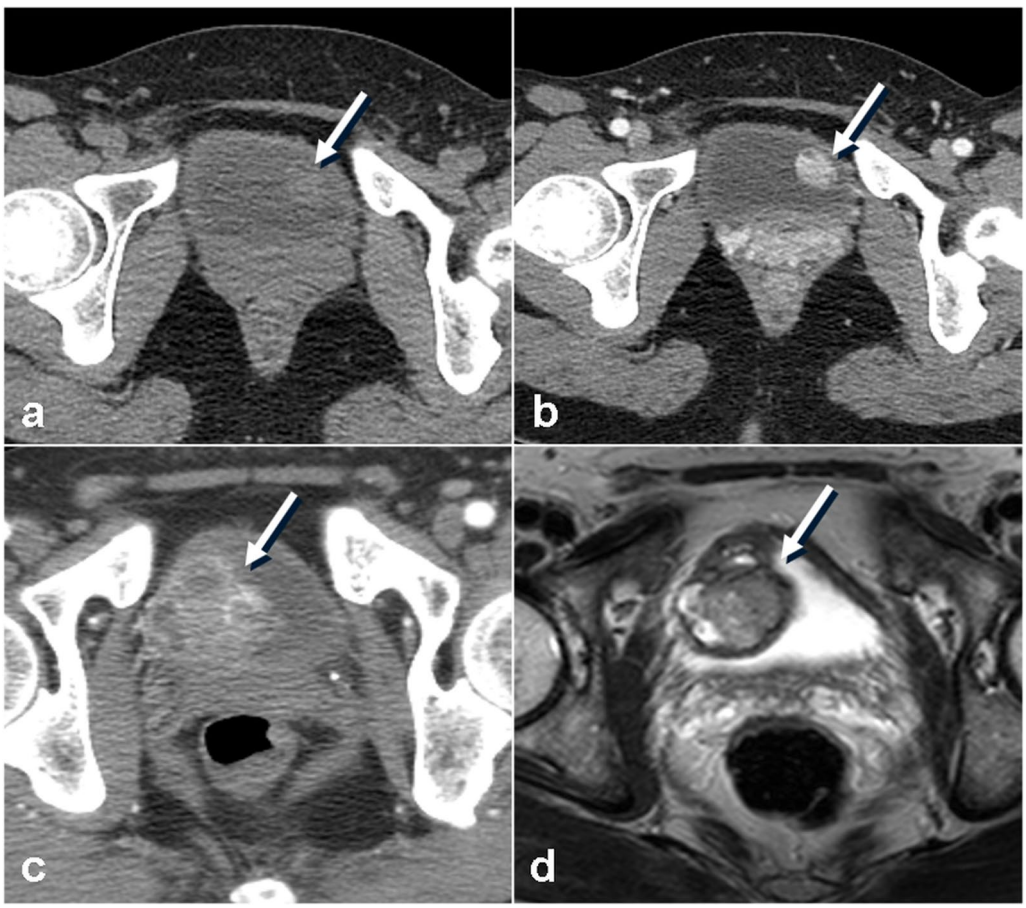

Fig. 11 Two cases of bladder paraganglioma. Axial pre-contrast (**a**) and post-contrast (**b**) CT images of a 38-year-old female woman showing a well-circumscribed, avidly enhancing nodular lesion at the anterior wall of the bladder. **c** Axial contrast-enhanced CT image of a 48-year-old man showing a lobulated intraluminal mass with heterogeneous early enhancement. **d** Axial T2-weighted MRI showing heterogeneous high signal intensity in the mass with a peripheral hypointense rim representing the calcification component

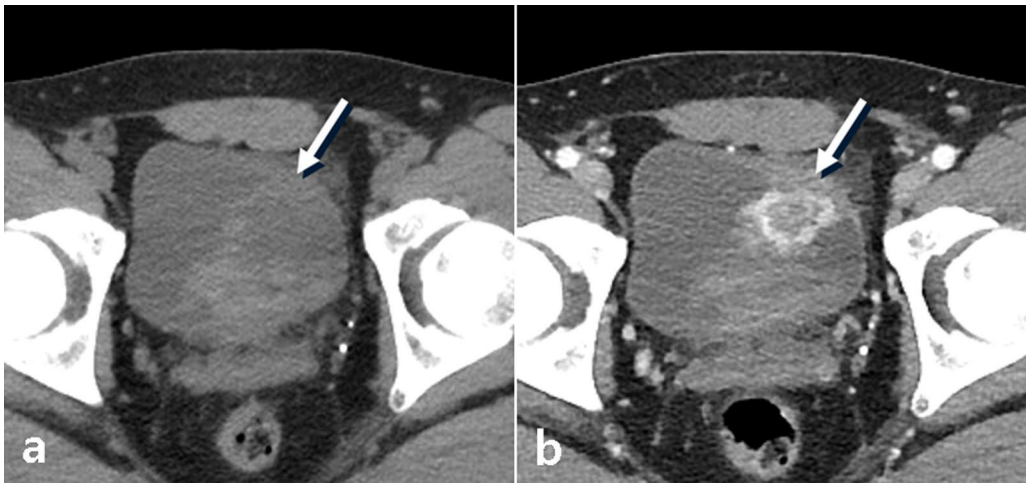

Fig. 12 A 40-year-old male patient with an inflammatory myoblastic tumor of the bladder. Axial pre-contrast (**a**) and post-contrast (**b**) CT images showing a single poorly marginated intraluminal polypoid mass with avid ring enhancement (arrow)

ring enhancement may be valuable in the diagnostic imaging of bladder IMTs [14, 19].

Solitary fibrous tumor

Solitary fibrous tumors are extremely rare mesenchymal neoplasms with fibroblast differentiation. They are more common in males and those aged 42–67 years [10].

On CT and MRI, solitary fibrous tumors appear as well-demarcated, solid, polypoid intraluminal or submucosal enhancing masses (Fig. 13). The presence of prominent feeding vessels or a vascular pedicle, although not specific, is a useful distinguishing feature [10].

Acute bacterial cystitis

Acute bacterial cystitis is more common in females and is usually caused by Escherichia coli. Patients with acute uncomplicated bacterial cystitis are readily diagnosed by history, clinical examination, and laboratory findings without the need for secondary CT [7].

Patients with acute bacterial cystitis often have normal CT findings but may show diffuse bladder wall thickening, mucosal irregularity, enhancement, and mural hypertrophy due to severe mucosal edema and fold thickening (Fig. 14) [2, 7, 20]. Furthermore, pseudotumors and focal protrusions can sometimes be observed. If severe infection and inflammation progress chronically, bladder

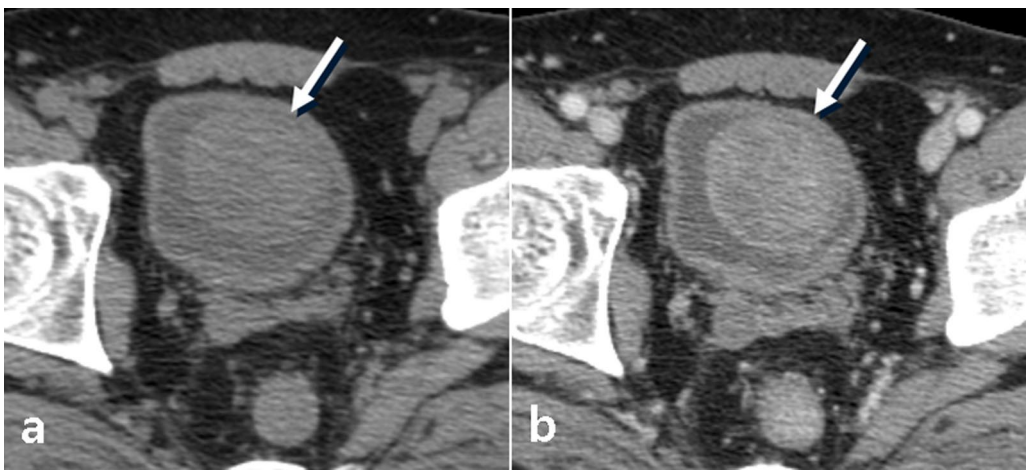

Fig. 13 A 49-year-old male patient with a solitary fibrous tumor of the bladder. Axial pre-contrast (**a**) and post-contrast (**b**) CT images showing a large well-circumscribed solid enhancing mass (arrow) in the bladder

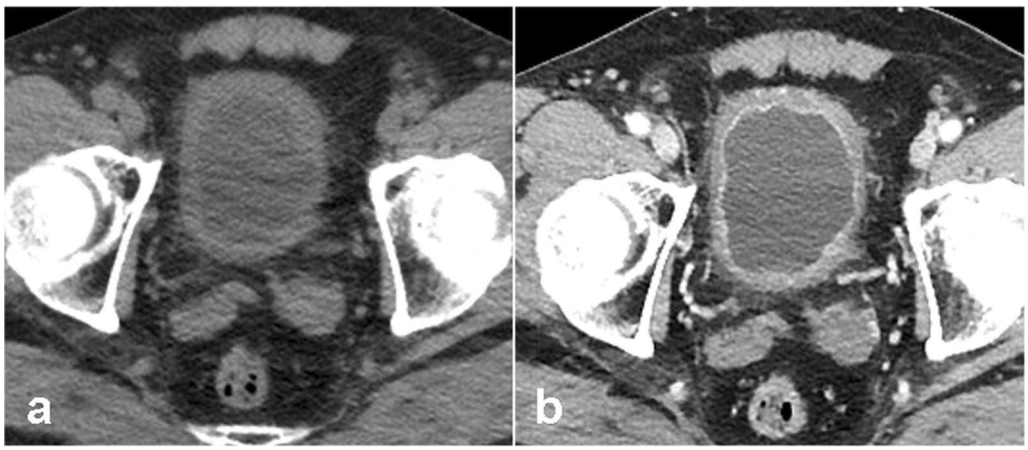

Fig. 14 A 62-year-old female patient with acute bacterial cystitis. Axial pre-contrast (**a**) and contrast-enhanced (**b**) CT images showing diffuse enhancement of the mucosal surface with wall thickening of the bladder

volume may be reduced owing to fibrosis or contraction of the bladder wall [7, 20].

However, CT offers a more comprehensive anatomical and functional assessment of the upper and lower urogenital tract, a detailed assessment of renal function and excretion, and increased sensitivity for calculi and early gas-forming infections [7].

Eosinophilic cystitis

Eosinophilic cystitis is a rare chronic inflammatory disease of the bladder. It is characterized by an extensive local infiltrate of eosinophils into all layers of the bladder wall and is associated with variable degrees of fibrosis and muscle necrosis [14, 21]. The mean age at diagnosis has been reported to be 41.6 years, with equal distribution in both sexes [21].

The imaging findings are nonspecific, with focal or diffuse thickening of the bladder wall (Fig. 15), which can be difficult to differentiate from other types of cystitis and sometimes bladder cancer [14, 21].

Conclusions

MDCT plays a large role in the evaluation of patients with known and suspected bladder cancer. MDCT can be used as an initial bladder examination in such patients and can replace cystoscopy. A summary of the MDCT findings for bladder lesions is provided in Tables 2 and 3. The role of the radiologist is to ensure that broad spectrum bladder lesions are detected and diagnosed preoperatively if possible.

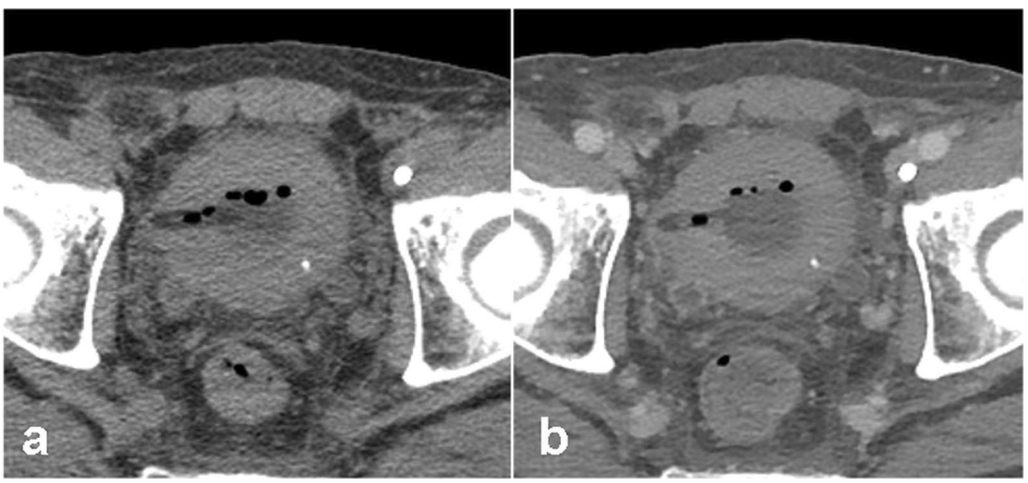

Fig. 15 A 65-year-old male patient with eosinophilic cystitis. Axial pre-contrast (**a**) and contrast-enhanced (**b**) CT images showing diffuse mural thickening of the bladder wall, which is nonspecific and difficult to distinguish from other cystitis or tumors

Table 2 Summary of the clinical and CT features of malignant bladder lesions

Bladder lesion	Clinical features	CT features
Bladder Cancer	Three main cell types: urothelial carcinoma, squamous cell carcinoma and adenocarcinoma Urothelial carcinoma: most common, 95%, multicentric (up to 40%)	Intraluminal papillary or nodular mass, asymmetric or focal wall thickening, small filling defects or less frequently diffuse wall thickening Squamous cell carcinoma: sessile rather than papillary Adenocarcinoma: diffuse bladder wall thickening and perivesical fat stranding
Leiomyosarcoma	< 1% of all bladder malignancies Risk factors: systemic chemotherapy with cyclophosphamide and radiation therapy	Poorly circumscribed margin and invasion of the adjacent structure
Rhabdomyosarcoma	Most common bladder tumor in children (< 10 years) Male: female ratio 1:3	Large, nodular filling defects or masses in a polypoid or grape-like shape
Lymphoma	Primary lymphoma is extremely rare Secondary involvement in 10%–25% MALT or DLBCL > 60 years	Nonspecific: solitary bladder masses (70%), multiple masses (20%) and diffuse bladder wall thickening (10%)

CT—computed tomography; MALT—mucosa-associated lymphoid tissue; DLBCL—diffuse large B-cell lymphoma

Table 3 Summary of the clinical and CT features of benign bladder lesions

Bladder lesion	Clinical features	CT features
Leiomyoma	< 0.5% among all types of bladder tumors Most common in those approximately 50 years of age Intravesical (60%, symptomatic), intramural (10%), or extravesical (30%)	Well-delineated, smooth, and uniform solid mass of the bladder wall Like those of uterine leiomyoma Cystic component indicating degeneration
Papilloma and PUNLMP	Papillary lesions of the bladder urothelium PUNLMP: low-grade, small, solitary neoplasm with no invasion or metastasis Surveillance is required (recurrence and progression)	Polypoid enhancing lesion and filling defect Difficult to distinguish from low-grade carcinoma
Cystitis Cystica and Cystitis Glandularis	Chronic inflammatory disorders Association with metaplasia incited by chronic irritation or infection Predominantly occur at the bladder neck and trigone	Single or multiple masses that are variable in number and size May result in a cobblestone pattern
Endometriosis	Only premenopausal women Posterior wall of the bladder, including the dome, trigone, or vesicouterine pouch	Typically, a submucosal mass, located posteriorly in the bladder, obtuse bulge into the lumen Other endometriosis foci in the pelvis
Paraganglioma	< 6% of all paragangliomas < 0.06% of all primary bladder tumors Most common in those aged 30–50 years, sporadic occurrence (mostly) Hereditary syndrome (neurofibromatosis, von Hippel–Lindau and Sturge–Weber syndrome) Characteristic 'micturition attack' Functional paraganglioma (> 3 cm)	Well-marginated, submucosal, solid solitary mass Most common in the dome or the trigone of the bladder Attach to the bladder wall with a broad base
Inflammatory Myoblastic Tumor	Spectrum of nonneoplastic myofibroblastic proliferation with inflammatory infiltrates and myxoid components Younger individuals, particularly female patients Associated with a history of undergoing pelvic surgery	Single intraluminal or exophytic bladder mass May be ulcerated or show ring enhancement Superior wall or the front wall of the bladder
Solitary Fibrous Tumor	More common in males Most common in those aged 42–67 years	Well-demarcated, solid, polypoid intraluminal or submucosal enhancing masses Presence of prominent feeding vessels or a vascular pedicle
Acute Cystitis	More common in females Usually caused by Escherichia coli Diagnosed by history, clinical exam, and laboratory findings	Diffuse bladder wall thickening, mucosal irregularity, enhancement, and mural hypertrophy Sometimes a pseudotumor or focal protrusion Chronic state: bladder volume may be reduced due to fibrosis or contraction of the bladder wall
Eosinophilic Cystitis	Rare chronic inflammatory disease of the bladder Extensive local infiltrate of eosinophils into all layers of the bladder wall	Nonspecific with focal or diffuse bladder wall thickening

Abbreviations

MDCT	Multidetector computed tomography
CT	Computed tomography
MPR	Multiplanar reformation
MRI	Magnetic resonance imaging
VI-RADS	Vesical imaging-reporting and data system
MALT	Mucosa-associated lymphoid tissue
DLBCL	Diffuse large B-cell lymphoma
PUNLMP	Papillary urothelial neoplasms of low malignant potential
IMT	Inflammatory myoblastic tumor
WHO	World Health Organization

Acknowledgments
Not Applicable.

Author contributions
Park SB took a conception and design for this study. Lee ES and Park HJ acquired the data for this study. Yoon JW, Lee ES and Park HJ analyzed and interpreted the patient data regarding bladder CT. Yoon JW drafted the manuscript. Park SB revised the manuscript and supervised this study thoroughly. All authors have read and approved the final manuscript.

Funding
This research did not receive any specific grant from funding agencies in the public, commercial or not-for-profit sectors.

Availability of data and materials
Data are available on request due to privacy or other restrictions.

Declarations

Ethics approval and consent to participate
This study has been approved by the institutional review board. This article does not contain any studies with human participants performed by any of the authors.

Consent for publication
Informed consent was waived from all patients for being included in the study.

Competing interests
The authors declare that they have no competing interests.

Received: 11 December 2022 Accepted: 5 February 2023
Published online: 14 February 2023

References

1. Han BH, Park SB, Chang IH, Chi BH, Park HJ, Lee ES (2021) Urothelial-phase thin-section MDCT of the bladder in patients with hematuria: added value of multiplanar reformatted images. Abdominal Radiol 46:2025–2031
2. Abouelkheir RT, Abdelhamid A, Abou El-Ghar M, El-Diasty T (2021) Imaging of bladder cancer: standard applications and future trends. Medicina (Kaunas) 57:220
3. Helenius M, Dahlman P, Lonnemark M, Brekkan E, Wernroth L, Magnusson A (2016) Comparison of post contrast CT urography phases in bladder cancer detection. Eur Radiol 26:585–591
4. Amin MF, Abd El Hamid AM (2013) The diagnostic accuracy of multidetector computed tomography with multiplanar reformatted imaging and virtual cystoscopy in the early detection and evaluation of bladder carcinoma: comparison with conventional cystoscopy. Abdom Imaging 38:184–192
5. Cohan RH, Caoili EM, Cowan NC, Weizer AZ, Ellis JH (2009) MDCT urography: exploring a new paradigm for imaging of bladder cancer. AJR Am J Roentgenol 192:1501–1508
6. Trinh TW, Glazer DI, Sadow CA, Sahni VA, Geller NL, Silverman SG (2018) Bladder cancer diagnosis with CT urography: test characteristics and reasons for false-positive and false-negative results. Abdom Radiol (NY) 43:663–671
7. Hirshberg B, Rheinboldt M (2020) MDCT imaging of acute bladder pathology. Curr Probl Diagn Radiol 49:422–430
8. WHO (2022) WHO classification of tumours: urinary and male genital tumours, 5th ed, vol 8. International Agency for Research on Cancer
9. Song W, Jeon HG, Jeong BC et al (2017) Clinical significance of incidentally detected bladder wall thickening on computed tomography. Int Urol Nephrol 49:191–196
10. Wong-You-Cheong JJ, Woodward PJ, Manning MA, Sesterhenn IA (2006) Neoplasms of the urinary bladder: radiologic-pathologic correlation. Radiographics 26:553–580
11. Naik N, Lin M, Lin P (2018) Genitourinary involvement of lymphomas on FDG-PET. Br J Radiol 91:20170273
12. Zachariou A, Filiponi M, Dimitriadis F, Kaltsas A, Sofikitis N (2020) Transurethral resection of a bladder trigone leiomyoma: a rare case report. BMC Urol 20:152
13. Humphrey PA, Moch H, Cubilla AL, Ulbright TM, Reuter VE (2016) The 2016 WHO classification of tumours of the urinary system and male genital organs-part B: prostate and bladder tumours. Eur Urol 70:106–119
14. Wong-You-Cheong JJ, Woodward PJ, Manning MA, Davis CJ (2006) Inflammatory and nonneoplastic bladder masses: radiologic-pathologic correlation. Radiographics 26:1847–1868
15. Potts S, Calleary J (2017) Cystitis cystica as a large solitary bladder cyst. J Endourol Case Rep 3:34–38
16. Yuan Y, Su Z, Zhu R, Li X, Xu G (2021) Bladder paraganglioma: three cases report and literature review. Int Med Case Rep J 14:765–771
17. Zhang J, Bai X, Yuan J et al (2021) Bladder paraganglioma: CT and MR imaging characteristics in 16 patients. Radiol Oncol 56:46–53
18. Chen B, Li S, Fang X et al (2020) Inflammatory myofibroblastic tumor of the urinary system on computed tomography at a high-volume institution in China. Urol Int 104:960–967
19. Liang W, Zhou X, Xu S, Lin S (2016) CT manifestations of inflammatory myofibroblastic tumors (inflammatory pseudotumors) of the urinary system. AJR Am J Roentgenol 206:1149–1155
20. Steinkeler JA, Sun MRM (2017) Imaging of infections of the urinary and male reproductive tracts. Semin Roentgenol 52:83–89
21. Runge SB, Hoyer S, Winding L (2016) Macroscopic hematuria and a bladder mass: eosinophilic cystitis in a 7-year-old boy. Case Rep Radiol 2016:9346218

Publisher's Note